Published in final edited form as:
Biochem Insights. 2010 September 1; 2010(3): 47–59. doi:10.4137/BCI.S5340.

Morphological Changes and Immunohistochemical Expression of RAGE and its Ligands in the Sciatic Nerve of Hyperglycemic Pig (*Sus Scrofa*)

Judyta K. Juranek[1], **Alexey Aleshin**[1], **Eileen M. Rattigan**[2], **Lynne Johnson**[2], **Wu Qu**[1], **Fei Song**[1], **Radha Ananthakrishnan**[1], **Nosirudeen Quadri**[1], **Shi Du Yan**[1], **Ravichandran Ramasamy**[1], **Ann Marie Schmidt**[1], and **Matthew S. Geddis**[1,3]

[1]Division of Surgical Science, Columbia University Medical Center, New York, NY, 10032, USA.

[2]Division of Cardiology, Columbia University Medical Center, New York, NY, 10032, USA.

[3]Department of Science, BMCC-City University of New York, New York, NY, 10007, USA.

Abstract

The aim of our project was to study the effect of streptozotocin (STZ)—induced hyperglycemia on sciatic nerve morphology, blood plasma markers and immunohistochemical expression of RAGE (the Receptor for Advanced Glycation End-products), and its ligands—S100B and Carboxymethyl Lysine (CML)-advanced glycation endproduct (AGE) in the laboratory pig. Six months after STZ —injections, blood plasma measurements, morphometric analysis of sciatic nerve fiber density, immunofluorescent distribution of potential molecular neuropathy contributors, ELISA measurement of plasma AGE level and HPLC analysis of sciatic nerve levels of one of the pre-AGE and the glycolysis intermediate products—methyl-glyoxal (MG) were performed. The results of our study revealed that STZ—injected animals displayed elevated levels of plasma glucose, gamma glutamyl transferase (GGT) and triglycerides. The sciatic nerve of STZ-injected pigs revealed significantly lower numbers of small-diameter myelinated fibers, higher immunoreactivity for RAGE and S100B and increased levels of MG as compared to control animals. Our results correspond to clinical findings in human patients with hyperglycemia/diabetes-evoked peripheral neuropathy and suggest that the domestic pig may be a suitable large animal model for the study of mechanisms underlying hyperglycemia-induced neurological complications in the peripheral nerve and may serve as a relevant model for the pre-clinical assessment of candidate drugs in neuropathy.

Keywords

pig; sciatic nerve; RAGE; AGE; S100B; CML

Corresponding author jkj2110@columbia.edu; jkj2110@gmail.com.

Disclosures

This manuscript has been read and approved by all authors. This paper is unique and not under consideration by any other publication and has not been published elsewhere. The authors and peer reviewers report no conflicts of interest. The authors confirm that they have permission to reproduce any copyrighted material.

Introduction

Metabolic and morphological changes in peripheral nerves are the most common nervous system complications in patients with diabetes, often leading to the development of a diabetic polyneuropathy (DPN), predominately affecting sensory and autonomic function of peripheral nerves.[1–3] The molecular mechanisms underlying the pathogenesis of these diabetes related changes are not yet fully understood, but lack of neurotrophic support,[4] oxidative stress, activation of Protein Kinase C (PKC) pathway and enhanced protein glycation leading to accumulation of Advanced Glycation End-products (AGEs)[5–7] are among the major causes of neuronal dysfunction. AGEs, among which carboxymethyllysine (CML)—AGE group is most common, are heterogeneous class of molecules modifying cellular function by an array of distinct mechanisms, including ligation and activation of the signal transduction receptor, RAGE (Receptor for Advanced End-Glycation products).[7] Extensive studies on RAGE and its function in hyperglycemia/diabetes conducted in STZ-induced type 1 diabetes small animal models have shown that RAGE is upregulated in diabetic tissues such as heart, retina and peripheral nerve, affecting the function of these organs and subsequently leading to the development of atherosclerosis and peripheral neuro-, retino- and nephropathy.[8,9] Furthermore, it has been shown that the activation of RAGE by one of its ligands, S100B, a calcium binding protein and glial/Schwann cell marker, in dorsal root ganglion (DRG) cultures increases cellular oxidative stress, resulting in sensory neuron injury, neuronal apoptosis and nerve dysfunction, factors likely contributing to the development of peripheral neuropathy.[10] Additionally, it has been noted that the expression of S100B is elevated in neurodegenerative disorders and acute brain injuries, making this protein a potential biomarker and possible modulator of nervous system injury.[11,12] In our study, we have focused on establishing the morphological and molecular evidence of peripheral nervous system diabetic complications in the pig, taking advantage of its close physiological resemblance with the human organism.[13]

Particularly in the field of diabetes, the pig has gained considerable interest, as its metabolic, biochemical and pathophysiological responses to the disease mimic in part those observed in humans.[14,15] It has been shown that blood supply of the porcine pancreas is similar to that of human pancreas and the number of beta-cells is within similar range as observed in humans making in a valuable model for the study of diabetes. The most stable and commonly accepted pig model of diabetes is STZ-induced type 1 diabetes *(diabetes mellitus)*,[14,15] where glucose metabolism and insulin secretion remain at the very similar level as in human diabetic patients. To date, the type 1 STZ-induced hyperglycemic/diabetic pig model has been predominately validated in studies of the cardiovascular complications of the disease[16–18] while neuronal complications in this model are unclear. Thus, the aim of this paper is to extend the body of research in this, latter, area as well as provide novel data on distribution of RAGE and its binding partners in peripheral nervous system in the hyperglycemic pig.

Materials and Methods

Animals

Twelve juvenile castrated male Yorkshire pigs, weighing from 17.1 kg to 23.2 kg, (ABI, Inc. Danboro, PA, USA) were used in this study. The pigs were divided into two groups—six diabetic and six control—and were individually housed in enriched environment cages. Prior to the experiment initiation, the pigs were given one week of acclimatization to observe their general health, to minimize physiological stress and to ensure proper conduct of the study. After acclimatization, hyperglycemia was induced as previously described.[19] Briefly, animals were anesthetized and injected intravenously with 50 mg/kg sterile streptozotocin (STZ) solution in citrate buffer (100 mM, pH 4.5; Sigma, St. Louis, MO, USA) for three

consecutive days while control pigs were injected with equal amounts of vehicle (citrate buffer). During induction of hyperglycemia, experimental pigs were fed normal chow supplemented with dextrose (2× per day, 25 g, Sigma, St. Louis, MO, USA) to offset the anticipated insulin release. Afterwards they were fed a 10% high fat, 1.5% high cholesterol diet (Harlan Tekland, Madison, WI, USA) to mimic diabetic hyperlipidemia. The control pigs remained on a normal chow diet throughout the whole time of the experiment. One of the six experimental pigs required treatment with insulin glargine (0.2 mg/kg, Sanofi-Aventis, Bridgewater, NJ, USA) subcutaneously once daily to prevent recurrent diabetic ketoacidosis for the last 12 weeks of the experiment. At administered doses of insulin, blood glucose levels were maintained at hyperglycemic values above 20 mmol/l until sacrifice. Due to the space limits, control animals were sacrificed four weeks before diabetic animals. The experimental pigs were sacrificed 6 months after induction of hyperglycemia. All animal procedures were performed in accordance with the Principles of Laboratory Animal Care (NIH publication no. 85-23, rev. 1985) and were approved by the Columbia University Institutional Animal Care and Use Committee.

Physiological status and general health condition evaluation

Plasma glucose levels were measured prior to the experiment initiation, 7 days after the first STZ injection and then once per month for the duration of the experiment using a hand-held glucometer. Glucose levels were monitored monthly until the end of the experiment or when indicated by a change in the clinical status of the pig. To assess physiological status and to evaluate the general condition of animals, weight measurement and routine blood tests for hemoglobin, blood urea nitrogen (BUN), gamma glutamyl transferase (GGT), creatinine, cholesterol and triglyceride were performed on the initial day of the experiment, and at 4, 8, 12 and 24 weeks after hyperglycemia induction.

Methyl-glyoxal (MG) measurement

Extracts of sciatic nerve (50–70 mg) from control and hyperglycemic animals were collected on the final day of the experiment, digested with perchloric acid (0.5 M) and the neutralized supernatant was derivatized to 2-methylquinoxaline (MQ, 1:1) as previously described.[20] Levels of MG were then indirectly measured by determining the levels of MQ by HPLC at 335 nm.

AGE measurement

Establishment of AGE baseline level was conducted on the day of experiment initiation and blood AGE levels were measured 3 and 6 months after the hyperglycemia induction. Briefly, samples were prepared according to standard protocol,[21] transferred onto 96 well plates, blocked for 1 h at room temperature in blocking buffer (5% GSA, 1% BSA in 0.1 M PBS, pH 7.4) and incubated for 3 h at room temperature with an affinity-purified chicken antibody against AGEs diluted 1:100 in blocking buffer.[22] After primary antibody incubation, samples were washed several times with PBS and subsequently incubated with goat anti-chicken IgG at 1:10,000 dilution in blocking buffer, developed and read by spectrophotometer at 490 nm. Results were given in arbitrary AGE units (AAU), as previously described.[21]

Morphological analysis of peripheral nerve changes

Animals were euthanized by intravenous pentobarbital injections (Euthasol, 120 mg/kg, Henry Schein, Melville, NY, USA). A longitudinal skin incision at the upper hindlimb level with blunt separation of gluteal muscles was performed to expose the sciatic nerve and 10 mm long nerve fragments were collected. After collection, samples were immediately transferred to fixative (2.5% glutaraldehyde and 2% paraformaldehyde (PFA) in 0.1 M PBS,

pH 7.4) and stored at 4 °C until further processing. For morphological analysis, samples were postfixed in 1% osmium tetroxide (0.1 M Phosphate Buffer), dehydrated with serial washing in ethanol (50%, 75%, 95% −2 × 10 min and 100% −3 × 10 min), infiltrated with propylene oxide (1–2 hr) and embedded in low viscosity epoxy medium (Spurr, Electron Microscopy Sciences, Hatfield, PA, USA). Cross sections were cut at 0.5 μm thickness using a 2088 ultratome (LKB Produkter AB, Bromma, Sweden), stained with toluidine blue and examined with an Axioscope 2 Plus microscope (Zeiss, Thornwood, NY, USA). Images were captured using the Axiovision computer analysis system (Zeiss, Thornwood, NY, USA) connected to CCD Axiocam video camera. The myelinated fiber density quantification was performed using ImageJ 7.1 (NIH open source software, USA) with Cell Counter plug-in. One cross section of sciatic nerve fascicule from five control and five diabetic animals was analyzed. Within one cross section, three fascicles, largest, medium and the smallest, fitting into 400 × 400 μm square, were selected for quantification to ensure proper counting methodology.[23–25] Discrimination between small (3.3–3.7 μm Ø) and large (11.2–21.6 μm Ø) fibers was set manually and standardized in all studied samples.

Immunofluorescence (IF)

Sciatic nerve samples from diabetic and control animals (euthanasia procedure as previously described) were collected, transferred to fixative (4% PFA in destilled H_2O) for 12 h, cryoprotected in 20% sucrose solution for 24 h, mounted in optimal cutting temperature compound (Tissue-Tek O.C.T., Sakura Finetek, Zoeterwoude, Netherlands) and stored at −20 °C for further processing. Alternatively, collected samples were immediately snap-frozen in liquid nitrogen and stored in −80 °C without prior fixation. Frozen samples were cut transversely and longitudinally at 10 μm thickness on a cryostat (Microm HM 550, Thermo Scientific, Waltham, MA, USA) and collected on polylysine coated slides (SuperFrost Plus, Fisher Scientific, Pittsburgh, PA, USA), always in the same order—1st series with two diabetic and two control sections from 4 different animals in total and 2nd series with 4 sections (control or diabetic) from 1 animal, to ensure similar staining condition and to minimize risk of false positive or false negative results. After slide collection, PFA-fixed sections were allowed to dry for 30 min at room temperature, while non-fixed sections were first transferred into containers with cold acetone, fixed for 5 min and then similar to PFA sections, and then they were allowed to dry for 30 min. Afterwards, all tissue sections were processed according to standard immunostaining protocol. In brief, dried sections were incubated with blocking solution (Cas-block, Invitrogen, Carlsbad, CA, USA) for 1 h, incubated in primary antibodies for 16 hours (for details, see antibody section), rinsed 4 × 5 min in PBS, incubated with secondary antibodies for 1 h, rinsed again for 4 × 5 min in PBS and mounted in fluorescent mounting medium (DAKO, Carpinteria, CA, USA). Mounted sections were allowed to stabilize for 30 min and afterwards were examined at 200x and 400x using a Scanning Confocal System (Bio-Rad Radiance 2000, Zeiss, Thornwood, NY, USA) attached to Nikon Eclipse 800 with krypton-argon and red diode lasers (excitation lines 488, 568, and 637 nm). Double immunostained images were acquired in a sequential mode to avoid bleed-through effect. All image acquisition parameters were kept identical for each studied specimen. To optimize the specificity of the labeling, the concentration of each primary antibody was tested in trial series ranging from 1:50 to 1:500 and the optimal dilution was used for experimental staining. To establish the specificity of the secondary antibodies, standard immunostaining procedure with omission or replacement of primary antibodies on sections from each sample was carried out parallel to the experimental staining. Quantification of immunofluorescent signal from control and hyperglycemic tissues single stained for RAGE and its ligands CML and S100B was calculated using ImageJ histogram function for RGB images and obtained as mean grey value of pixels per selected region of interest[26] given in arbitrary units (IAU). Colocalization percentage of RAGE positive fibers double stained for ligands and markers was calculated

manually using ImageJ Cell Counter Plugin, where number of RAGE positive fibers was used as a reference number (100% of all positive fibers).

The following primary antibodies were used: polyclonal rabbit anti-RAGE and polyclonal anti-S100B generated as described earlier (Ma et al 2007), polyclonal goat anti-RAGE, 1:200 (GeneTex, Irvine, CA, USA); polyclonal rabbit anti-Vesicular Acetylocholine Transporter (VAChT), 1:500, rabbit anti-Tyrosine Hydroxylase (TH), 1:200, rabbit anti-Calcitonin Gene Related Peptide (CGRP), 1:200, monoclonal mouse anti-Macrophage Marker (MM, 25F9)—86 kD cell surface and cytoplasmic protein of mature human macrophages, 1:100 (Santa Cruz Biotechnology, Santa Cruz, CA, USA); polyclonal rabbit anti-Neurofilament (NF), 1:400 and polyclonal affinity purified anti-Munc13-1, 1:400 (Synaptic Systems, Goettingen, Germany. The following secondary antibodies were used: chicken anti-goat Alexa 568, 1:300, chicken anti-rabbit Alexa 488, 1:200 and Alexa 568, 1:300 and rabbit anti-mouse Alexa 488, 1:200 (Invitrogen, Carlsbad, CA, USA).

Statistics

Statistical analysis was performed using SPPS 13 (SPPS Inc., Chicago, IL, USA) or GraphPad, InStat (GraphPad Software, Inc., La Jolla, CA, USA). All values are presented as mean ± SEM. The statistical significance of differences was evaluated by ANOVA or Student's t-test as defined in the text.

Results

Plasma glucose level

The baseline plasma glucose level in animals measured before STZ treatment and the development of hyperglycemia was within standard reference values for the pig (2.91 ± 0.16 mmol/l). The significant 5.4 -fold (15.62 ± 0.87 mmol/l) increase in glucose level was already observed on the 7th day after STZ injection, followed by 7.8 fold increase (22.76 ± 1.27 mmol/l) 1 month after the injection. Monthly measurements performed until the final day of sacrifice revealed sustained, high levels of plasma glucose in the range of 22.6–25.42 mmol/l (Table 1). ANOVA and post-hoc Tukey-Kramer analysis revealed statistical significance between baseline and all further data point values ($P < 0.001$).

Physiological status and routine laboratory diagnostic marker evaluation

Routine health examination did not show any abnormalities throughout the entire period of the experiment. The initial weight of the experimental pigs was 19.73 ± 0.87 kg, increasing over the course of the experiment to a peak weight at 4 months of diabetes (27.6 ± 4.8 kg). Body weight subsequently declined to 20.4 ± 3.08 kg by the end of the experiment. Levels of Hb and BUN remained within normal reference values at all given time points, however there was a statistically significant progressive decline of Hb values over the duration of experiment (ANOVA, post-hoc Tukey-Kramer test, $P < 0.005$). Creatinine levels were slightly below reference values, but no statistical difference was noted between baseline and given data points. Additionally, there was a trend toward an increase in the levels of GGT and Triglyceride over the course of the experiment. Furthermore, significant increases in LDL and Cholesterol, between baseline and 3-month values were noted (ANOVA, post-hoc Tukey-Kramer test, $P < 0.005$) and for HDL between baseline and all studied time points. Diagnostic marker values for control animals remained within standard reference range throughout the entire duration of the experiment (Table 1).

Tissue Methyl-glyoxal and Plasma AGE measurement

HPLC analysis of sciatic nerve tissue revealed a low level of MG in control sciatic nerve tissue, ranging from 0.171 to 0.226 μm/g while in hyperglycemic sciatic nerve MG levels

were ~22 fold higher (range, 2.98–5.33 μm/g reaching statistical significance (ANOVA, post-hoc Tukey-Kramer test, $P < 0.05$) (Fig. 1A). As MGs are pre-AGE species, we examined levels of circulating AGEs in the plasma of diabetic animals and observed a trend toward a gradual increase in plasma AGE levels in the diabetic pigs. The baseline plasma AGE level was established prior to the experiment, estimated as 57.55 ± 5.82 AAU. At 3 months after STZ injection, plasma AGE level reached 75.33 ± 24.34 AAU, and at 6 months 118.45 ± 50.35 AAU (~2 fold increase) (Fig. 1B).

Morphological analysis of peripheral nerves

Noticeable loss of small diameter myelinated fibers and some morphological changes were observed in sciatic nerve structure of diabetic animals (Fig. 2B, A respectively). The overall density of myelinated fibers of diabetic pigs was lower compared to the control group (Fig. 2D, C respectively). The nerve morphology was evaluated based on the size of fiber diameter. The number of large diameter myelinated nerve fibers was similar between both groups (control, 898.54 ± 70.57 per mm vs. hyperglycemic, 1,001.04 ± 113.49 per mm). However, the number of small diameter myelinated fibers was significantly lower (~19%) in hyperglycemic samples (control 332.29 ± 19.83 vs. diabetic 260.62 ± 22.42 per mm; Paired T-test, $P < 0.05$) (Fig. 2E).

Immunofluorescence

Assessment of single staining immunofluorescence signal revealed changes in immunohistochemical expression for RAGE (Fig. 3A, B) and one of its ligands, S100B (Fig. 3E, F), whereas CML (Fig. 3C, D) remained consistent between control and hyperglycemic nerve samples. Furthermore, quantification of double-stained fibers positive both for RAGE and marker proteins NF (Fig. 4A, B), VAChT (Fig. 5A, B), TH (Fig. 5C, D), CGRP (Fig. 5E, F), CML (Fig. 6A, B) and S100B (Fig. 6C, D) revealed variable colocalization patterns depending on the protein studied, demonstrating significantly higher number of RAGE positive fibers co-stained for NF (91% ± 5%, Fig. 4C), and lower number co-stained for TH (58% ± 2%, Fig. 5H), CGRP (42% ± 4%, Fig. 5I) and S100B (82% ± 12%, Fig. 6H) compared to the control animals. (paired T-test, $P < 0.05$). Macrophage Marker (MM) staining revealed a lack of macrophage positive signal in the control group, but distinct well defined perineurium staining in the diabetic group (Fig. 6E, F).

Discussion

Our study demonstrates that the porcine sciatic nerve after 6 months of sustained hyperglycemia exhibits alterations in fiber density often observed in human patients with long-term diabetes. In addition, the results of our study provide for the first time the preliminary evidence of the expression of RAGE and its ligands in the porcine peripheral nerves and provide insight into MG, AGE precursor, and AGE levels in nerve and circulating blood, respectively, of healthy and STZ-injected pigs. Expression of the studied proteins as well as the level of neural MG is noticeably higher in hyperglycemic tissues and an increased trend in plasma AGE level is observed during the course of disease. Furthermore, the results of the routine laboratory plasma lipid tests were consistent with the data obtained from human subjects, suggesting, as shown recently in hyperglycemic patients with diagnosed peripheral neuropathy, that elevated levels of plasma lipids correlate with progression of neurological changes and neuropathy under diabetic/hyperglycemic conditions.[27,28] The alteration of fiber density and morphology and significant loss of the small diameter fibers in the peripheral sciatic nerve are characteristic morphological signs of progressive neuropathy in human diabetic patients,[29,30] Until now, the data on early structural changes in the peripheral nerve of hyperglycemic/diabetic animals was by far limited to the studies on small animal models and therefore almost by definition redundant

as compared to studies on larger, closer genetically, anatomically and physiologically related species, often failing to replicate subtle, sub-clinical metabolic, biochemical and/or morphological changes.[31,32] As shown in studies on neuropathy in type 1 diabetic mouse, structural deficits and symptomatic manifestation of the developing neurological abnormalities are less prominent and often delayed, as compared to human subjects at the relative stage of the disease, thus fail to serve as a probe of early DBN manifestation. [33] Strikingly, in the same pig model investigations on retinal morphological aberrations revealed that, in correlation with our data, 6 months of sustained hyperglycemia results in basement membrane thickening further supporting the notion that the STZ-induced pig model might be a useful tool aimed at capturing early signs of metabolic and morphological disturbances evoked by chronically elevated level of glucose. It has been well established that sustained elevations of blood glucose levels affect and alter the physiology of many organs, leading indirectly to the peripheral nervous system malfunctions. Hyperglycemia-induced oxidative stress and the subsequent increase in free radical production leads to cellular dysfunction and neuronal cell loss both via activation of apoptosis or necrotic cell death. As reported in human studies, sensory and/or autonomic fibers are usually affected early in diabetic patients.[30] Very late evidence of sensory fiber dysfunction may be detected by standard neurological examination combined with physiological tests, but early onset of sensory dysfunction might be easily overlooked and/or masked by other symptoms of diabetes until patients develop severe, painful neuropathy, as pointed out in an earlier report.[34] Our morphological studies revealed a significant ~19% loss of small diameter fibers in the sciatic nerve at 6 months of hyperglycemia, which is the first detection of such loss reported to date in the peripheral nervous system in a large animal model. Similarly, a loss of cardiac nerve fibers was observed electrophysiologically in hyperglycemic pigs.[18] Our study supports the notion that observable loss of nerve fibers might be also influenced by the dietary regimen and hyperlipidemia, as reported in studies on obese human subjects[35] and observed in alimentary diabetes models in rodents.[36,37]

In addition to the morphological findings, our immunohistochemical studies demonstrate differential expression of RAGE and its two ligands in peripheral nerve tissue, previously not reported in this species and tissue. As observed in single and double staining images, RAGE immunofluorescence was more prominent in the hyperglycemic samples, present not only in the nerve itself but also in the surrounding vessels. Its expression in relation to neuronal marker, Neurofilament expressed by all fibers, revealed that in the control/healthy nerve tissue RAGE presence is confined rather to supportive cells than nerve fibers however as the co-staining with type- specific fiber markers revealed, the RAGE signal might be also detected in few motor, sensory or autonomic fibers. Hyperglycemic tissue staining revealed an increased presence of RAGE in all types of fibers and blood vessels which is consistent with previous reports on RAGE in murine diabetic tissues. RAGE, commonly linked and often cited as a molecule mediating and aggravating complications occurring in hyperglycemic states and inflammation disorders,[9] displayed increased expression levels based on immunohistochemical staining evaluation in the hyperglycemic vs. control nerve samples. It is well known that in several pathological states such as diabetes, atherosclerosis and neurodegenerative diseases, RAGE expression is elevated in response to the increased level of newly forming AGEs and other ligands.[9] Until now, increased expression of RAGE in the porcine peripheral nerve has not been shown. Taking into account available data obtained from our previous rodent studies and our current findings, a possible RAGE—ligand interaction metabolic pathway in diabetic neuropathy might be suggested. Briefly, RAGE-ligand interaction through intermediate signal transduction processes such as NF-$_K$B and MAP kinase pathways[38,39] may lead to increased cellular oxidative stress and thus contribute to nerve cell damage and dysfunction. Furthermore, it has been shown that genetic deletion of RAGE in mice correlates with lower expression of NF-$_K$B in sensory dorsal root ganglia (DRG) neurons, as well as in sensory sural nerve fibers.[34,40]

Interestingly, RAGE co-localization with its two ligands, CML and S100B, revealed that in control tissue there is a high degree of RAGE/ligand co-localization indicating that under physiological conditions, RAGE and its ligands are expressed at baseline levels in a limited numbers of nerve fibers and most likely interact with each other, producing RAGE-ligand complexes. In hyperglycemic tissue, there is a relevant increase in both CML and S100B expression, however the absolute value of co-localization of these two proteins with RAGE decreases, suggesting that both RAGE and its ligands may interact with other proteins as well. CML, one of the advanced glycation products and a biomarker of oxidative stress, accumulates at the higher rate in diabetes contributing along with other AGEs to the development of diabetes complications.[41] Furthermore, a recent report on CML showed that its accumulation is increased in aqueous humor of retina in diabetic patients and this increase correlates with the progression of retinopathy in those patients[42] suggesting, as observed in our study, that similar correlation might take place in pathogenesis of DPN. S100B has been demonstrated to exert, in nanomolar concentrations, a positive effect on axonal outgrowth, neuronal differentiation and survival during development and injury of peripheral nerves. However, higher micromolar concentrations of this protein and its binding to RAGE leads to neurotoxicity resulting in neuronal cell apoptosis, production of free radicals and caspase cascade activation in cultured cells.[43] S100B, apart from interacting with RAGE, has multiple binding domains through which it is able to interfere with cytoskeletal molecules and hence it may play an important role in events occurring at the axonal endings in normal and pathological conditions such as acute/chronic injury or neurodegenerative disorders.[44] Furthemore, increased observed macrophage positive cells around the hyperglycemic neural tissue confirmed an inflammatory status of hyperglycemic peripheral nerve suggesting the influence of RAGE on neuropathy from multiple sources.

In conclusion, our study addresses for the first time the state of the peripheral nerve in thehyperglycemic STZ-induced diabetic pig. Our results indicate that after 6 months of hyperglycemia, morphological aberrations of peripheral nerve fibers and noticeable loss of the small diameter fibers occur in the pig and suggest that STZ-injected pigs might serve as a relevant model in early studies of peripheral nerve changes under hyperglycemic conditions. Furthermore, our data reveals that levels of pre-AGE, AGEs and RAGE are modulated in the peripheral nerve of the STZ-injected pig in early-stage hyperglycemia. This finding provides background for more detailed studies on RAGE-ligand contribution to pathogenesis of peripheral nerve changes as well as reference data for further, pre-clinical studies on hyperglycemia-related neuronal changes in the species more closely related to humans.

Abbreviations

BUN	blood urea nitrogen
CGRP	Calcitonin Gene Related Peptide
CML	(DPN, diabetic peripheral neuropathy) Carboxymethyl Lysine
DPN	diabetic peripheral neuropathy
GGT	(DPN, diabetic peripheral neuropathy), gamma glutamyl transferase
MG	methyl-glyoxal
MQ	2-methylquinoxaline
PFA	paraformaldehyde
RAGE	Receptor for Advanced Glycation End-products

TH	Tyrosine Hydroxylase
VAChT	Vesicular Acetylocholine Transporter.

Acknowledgments

Authors would like to thank Dr. A. Hays for his helpful comments and critical review of the manuscript, G. Adist for his help with tissue collections, L. Woods for help with figure preparation, D. Babcock for linguistic comments, Y. Lu, K. Brown, L. Kelly and B. Kaplan for their excellent technical assistance. The study was supported by NIH grant no. AG026467-01 and AG17490.

References

1. Duby JJ, Campbell RK, Setter SM, et al. Diabetic neuropathy: an intensive review. Am J Health Syst Pharm. 2004; 61:160–176. [PubMed: 14750401]
2. Gregg EW, Sorlie P, Paulose-Ram R, et al. Prevalence of lower-extremity disease in the US adult population ≥ 40 years of age with and without diabetes: 1999–2000 national health and nutrition examination survey. Diabetes Care. 2004; 27:1591–1597. [PubMed: 15220233]
3. Sima AA, Kamiya H. Diabetic neuropathy differs in type 1 and type 2 diabetes. Ann N Y Acad Sci. 2006; 1084:235–249. [PubMed: 17151305]
4. Fernyhough P, Huang TJ, Verkhratsky A. Mechanism of mitochondrial dysfunction in diabetic sensory neuropathy. J Peripher Nerv Syst. 2003 Aug.:227–235. [PubMed: 14641647]
5. Singh R, Barden A, Mori T, et al. Advanced glycation end-products: a review. Diabetologia. 2001; 44:129–146. [PubMed: 11270668]
6. Sugimoto K, Yasujima M, Yagihashi S. Role of advanced glycation end products in diabetic neuropathy. Curr Pharm Des. 2008; 14:953–961. [PubMed: 18473845]
7. Yan SF, Ramasamy R, Schmidt AM. Mechanisms of disease: advanced glycation end-products and their receptor in inflammation and diabetes complications. Nat Clin Pract Endocrinol Metab. 2008; 4:285–293. [PubMed: 18332897]
8. Ramasamy R, Vannucci SJ, Yan SS, et al. Advanced glycation end products and RAGE: a common thread in aging, diabetes, neurodegeneration, and inflammation. Glycobiology. 2005; 15:16R–28R.
9. Yan SF, Ramasamy R, Schmidt AM. Receptor for AGE (RAGE) and its ligands-cast into leading roles in diabetes and the inflammatory response. J Mol Med. 2009; 87:235–247. [PubMed: 19189073]
10. Vincent AM, Perrone L, Sullivan KA. Receptor for advanced glycation end products activation injures primary sensory neurons via oxidative stress. Endocrinology. 2007; 148:548–558. [PubMed: 17095586]
11. Kleindienst A, Hesse F, Bullock MR, et al. The neurotrophic protein S100B: value as a marker of brain damage and possible therapeutic implications. Prog Brain Res. 2007; 161:317–325. [PubMed: 17618987]
12. Sen J, Belli A. S100B in neuropathologic states: the CRP of the brain? J Neurosci Res. 2007; 85:1373–1380. [PubMed: 17348038]
13. Swindle MM, Smith AC. Comparative anatomy and physiology of the pig. Scand J Lab Anim Sci. 1998; 25:11–21.
14. Larsen MO, Rolin B. Use of the Goettingen Minipig as a Model of Diabetes with Special Focus on Type 1 Diabetes Research. ILAR. 2004; 45:303–313.
15. Larsen MO, Wilken M, Gotfredsen CF, et al. Mild streptozotocin diabetes in the Gottingen minipig. A novel model of moderate insulin deficiency and diabetes. Am J Physiol Endocrinol Metab. 2002; 282 E1342–51.3.
16. Mésangeaua D, Laudeb D, Elghozib JL. Early detection of cardiovascular autonomic neuropathy in diabetic pigs using blood pressure and heart rate variability. Cardiovas Res. 2000; 45:889–899.
17. Fricker J. The pig: a new model of diabetic atherosclerosis. Drug Discov Today. 2001; 6:921–922. [PubMed: 11546599]

18. Arner RJ, Prabhu KS, Krishnan V, et al. Expression of myo-inositol oxygenase in tissues susceptible to diabetic complications. Biochem Biophys Res Commun. 2006; 339:816–820. [PubMed: 16332355]
19. Gerrity RG, Natarajan R, Nadler JL, et al. Diabetes-induced accelerated atherosclerosis in swine. Diabetes. 2001; 50:1654–1665. [PubMed: 11423488]
20. Ohmori S, Mori M, Kawase M, et al. Determination of methylglyoxal as 2-methylquinoxaline by high-performance liquid chromatography and its application to biological samples. J Chromatogr. 1987; 414:149–155. [PubMed: 3571379]
21. Schmidt AM, Vianna M, Gerlach M, et al. Isolation and characterization of two binding proteins for advanced glycosylation end products from bovine lung which are present on the endothelial cell surface. J Biol Chem. 1992; 267:14987–14997. [PubMed: 1321822]
22. Cellek S, Qu W, Schmidt AM, et al. Synergistic action of advanced glycation end products and endogenous nitric oxide leads to neuronal apoptosis in vitro: a new insight into selective nitrergic neuropathy in diabetes. Diabetologia. 2004; 47:331–339. [PubMed: 14676945]
23. Fazan VP, Salgado HC, Barreira AA. A descriptive and quantitative light and electron microscopy study of the aortic depressor nerve in normotensive rats. Hypertension. 1997; 30:693–698. [PubMed: 9323007]
24. Hunter DA, Moradzadeh A, Whitlock EL, et al. Binary imaging analysis for comprehensive quantitative histomorphometry of peripheral nerve. J Neurosci Methods. 2007; 166:116–124. [PubMed: 17675163]
25. Mayhew TM, Sharma AK. Sampling schemes for estimating nerve fibre size. I. Methods for nerve trunks of mixed fascicularity. J Anat. 1984; 139(Pt 1):45–58. [PubMed: 6381443]
26. Zhou X, Babu JR, da Silva S, et al. Unc-51-like kinase 1/2-mediated endocytic processes regulate filopodia extension and branching of sensory axons. Proc Natl Acad Sci U S A. 2007; 104:5842–5847. [PubMed: 17389358]
27. Tesfaye S, Chaturvedi N, Eaton SE, et al. Vascular risk factors and diabetic neuropathy. N Engl J Med. 2005; 352:341–350. [PubMed: 15673800]
28. Wiggin TD, Sullivan KA, Pop-Busui R, et al. Elevated triglycerides correlate with progression of diabetic neuropathy. Diabetes. 2009; 58:1634–1640. [PubMed: 19411614]
29. Mahmood D, Singh BK, Akhtar M. Diabetic neuropathy: therapies on the horizon. J Pharm Pharmacol. 2009; 61:1137–1145. [PubMed: 19703362]
30. Wong MC, Chung JW, Wong TK. Effects of treatments for symptoms of painful diabetic neuropathy: systematic review. BMJ. 2007; 335:87. [PubMed: 17562735]
31. Rogers CS, Stoltz DA, Meyerholz DK, et al. Disruption of the CFTR gene produces a model of cystic fibrosis in newborn pigs. Science. 2008; 321:1837–1841. [PubMed: 18818360]
32. Lunney JK. Advances in swine biomedical model genomics. Int J Biol Sci. 2007; 3:179–184. [PubMed: 17384736]
33. Toth C, Rong LL, Yang C, et al. Receptor for advanced glycation end products (RAGEs) and experimental diabetic neuropathy. Diabetes. 2008; 57:1002–1017. [PubMed: 18039814]
34. Singleton JR, Bixby B, Russell JW, et al. The Utah Early Neuropathy Scale: a sensitive clinical scale for early sensory predominant neuropathy. J Peripher Nerv Syst. 2008; 13:218–227. [PubMed: 18844788]
35. Straub RH, Thum M, Hollerbach C, et al. Impact of obesity on neuropathic late complications in NIDDM. Diabetes Care. 1994; 17:1290–1294. [PubMed: 7821169]
36. Obrosova IG, Ilnytska O, Lyzogubov VV, et al. High-fat diet induced neuropathy of pre-diabetes and obesity: effects of “healthy” diet and aldose reductase inhibition. Diabetes. 2007; 56:2598–2608. [PubMed: 17626889]
37. Russell JW, Berent-Spillson A, Vincent AM, et al. Oxidative injury and neuropathy in diabetes and impaired glucose tolerance. Neurobiol Dis. 2008; 30:420–429. [PubMed: 18424057]
38. Taguchi A, Blood DC, Del Toro G, et al. Blockade of RAGE-amphoterin signalling suppresses tumour growth and metastases. Nature. 2000; 405:354–360. [PubMed: 10830965]
39. Yan SD, Schmidt AM, Anderson GM, et al. Enhanced cellular oxidant stress by the interaction of advanced glycation end products with their receptors/binding proteins. J Biol Chem. 1994; 269:9889–9897. [PubMed: 8144582]

40. Bierhaus A, Haslbeck KM, Humpert PM, et al. Loss of pain perception in diabetes is dependent on a receptor of the immunoglobulin superfamily. J Clin Invest. 2004; 114:1741–1751. [PubMed: 15599399]

41. Shaw JN, Baynes JW, Thorpe SR. N epsilon-(carboxymethyl)lysine (CML) as a biomarker of oxidative stress in long-lived tissue proteins. Methods Mol Biol. 2002; 186:129–137. [PubMed: 12013760]

42. Ghanem AA, Elewa A, Arafa LF. Pentosidine and N-carboxymethyl-lysine: biomarkers for type 2 diabetic retinopathy. Eur J Ophthalmol. 2010

43. Huttunen HJ, Kuja-Panula J, Sorci G, et al. Coregulation of neurite outgrowth and cell survival by amphoterin and S100 proteins through RAGE activation. J Biol Chem. 2000; 275:40096–40105. [PubMed: 11007787]

44. Donato R. S100: a multigenic family of calcium-modulated proteins of the EF-hand type with intracellular and extracellular functional roles. Int J Biochem Cell Biol. 2001; 33:637–668. [PubMed: 11390274]

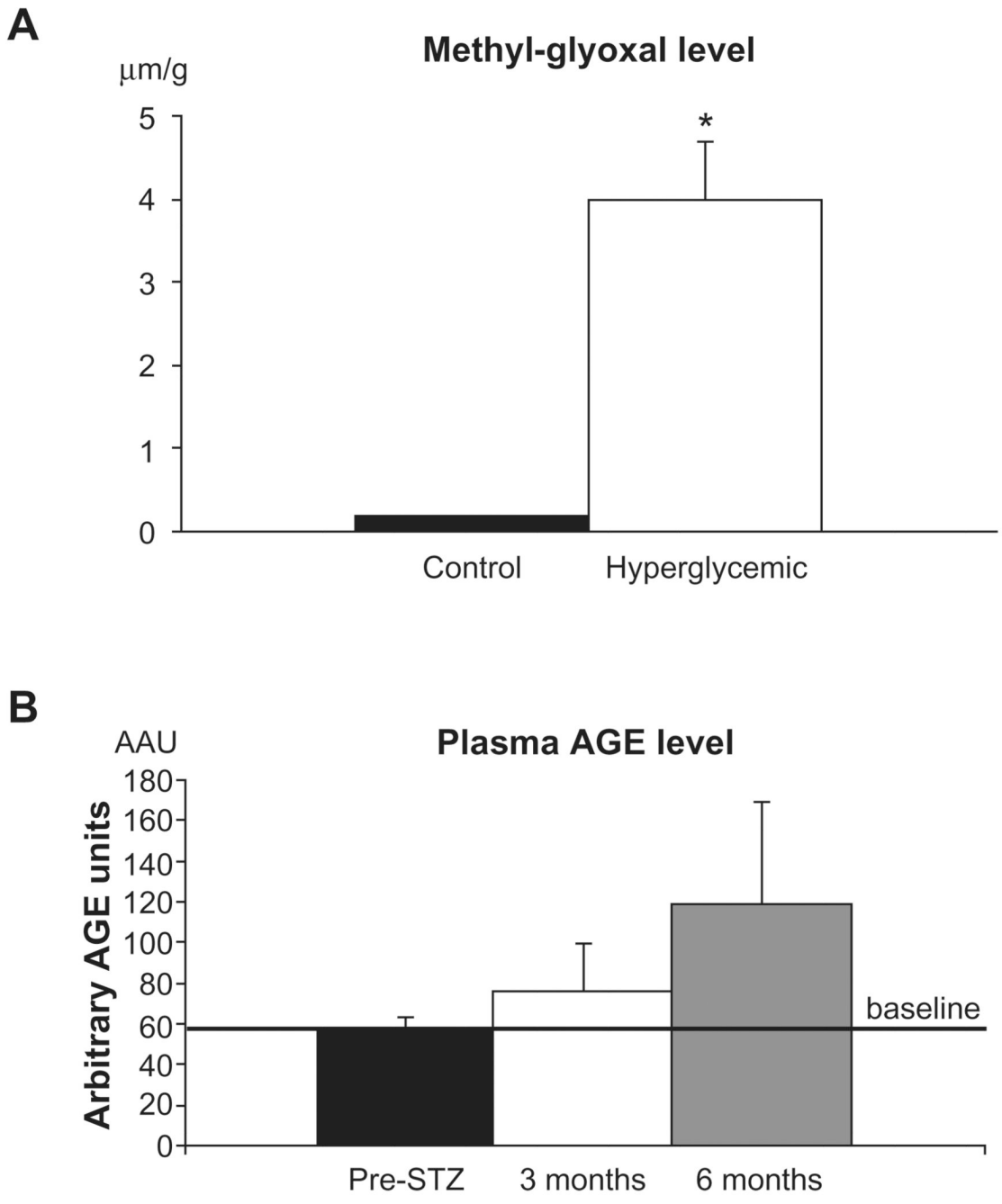

Figure 1.

A) Methyl-glyoxal levels in sciatic nerve tissue. Sciatic nerve tissue was retrieved and subjected to HPLC analysis for detection of levels of pre-AGE methyl-glyoxal (MG). As shown, hyperglycemic animals had significantly higher level of MG compared to the controls, $*P < 0.05$. **B**) Plasma AGE levels. AGE levels were measured by ELISA in the plasma and compared with the baseline level to determine the degree of glycation occurring during sustained hyperglycemia.

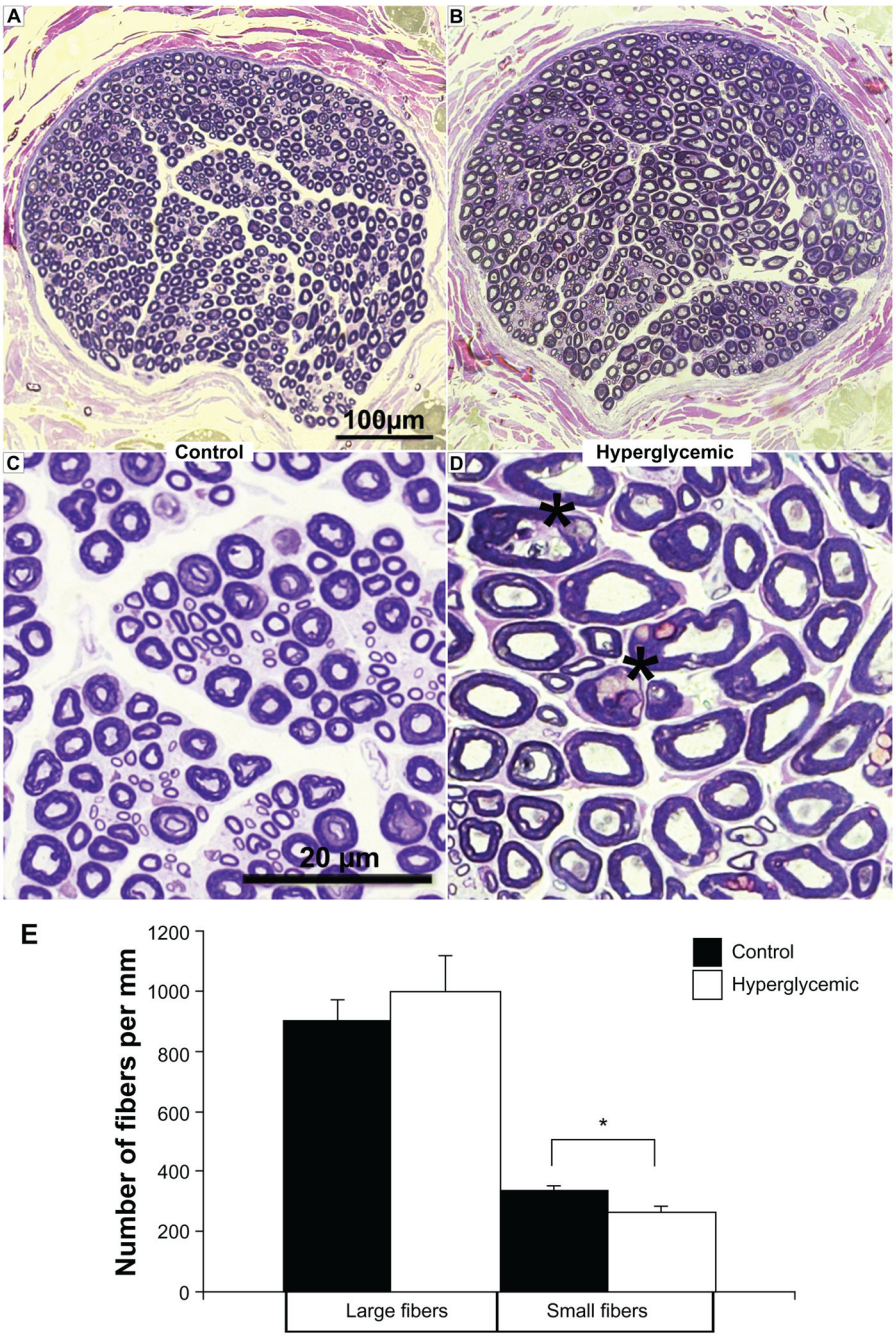

Figure 2.

A, B) Sciatic nerve morphometry. Semi-thin toluidine blue sections prepared from control pig sciatic nerve reveal a dense network of large diameter myelinated fibers motor and small diameter myelinated sensory regularly-shaped fibers, whereas sections from a hyperglycemic sciatic nerve reveal visible loss of small fibers; overall fiber morphology is altered suggesting the onset of sensorimotor neuropathy. **C, D**) Lower panel images magnify nerve morphology, displaying large and small fibers in the control sections and indicating increase in the number of irregular shaped fibers (asterisks) in the diabetic nerve. **E**) Quantification of fiber number was performed on the indicated sections and reported as values per mm. *$P < 0.05$.

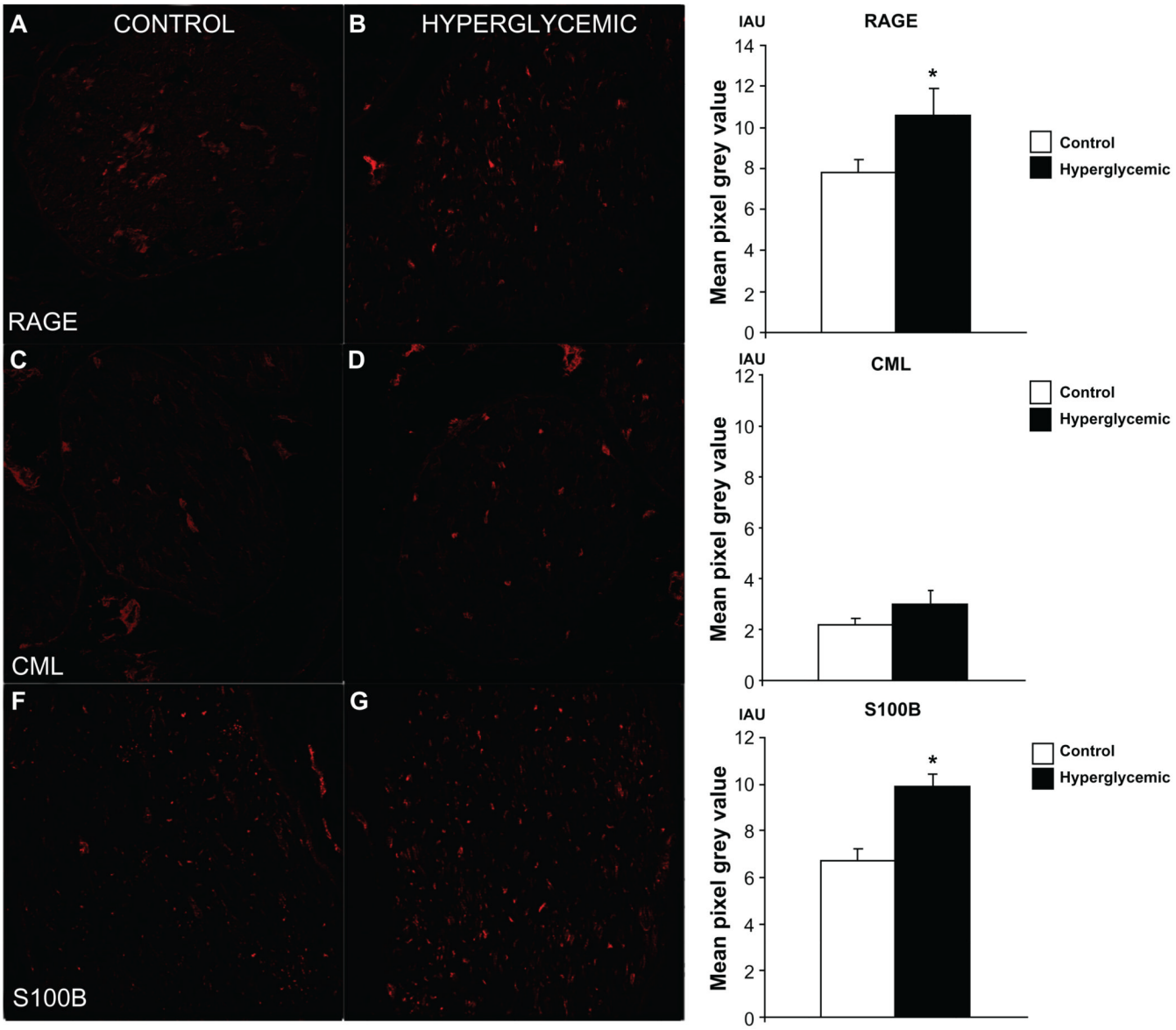

Figure 3.

Assessment of immunofluorescent signal in sciatic nerve sections single stained for RAGE and its ligands. Difference in immunofluorescent signal between control and hyperglycemic tissues was observed for RAGE (**A, B**) and S100B (**E, F**) indicating that under hyperglycemic conditions immunoexpression of these two proteins is increased. Level of CML (**C, D**) immunofluorescent signal was relatively low in both groups of animals and did not reach significant difference, however visible increase of CML positive fibers was noticed in hyperglycemic nerves suggesting that hyperglycemia likely induces immunoexpression changes of AGEs in the peripheral nerve over long period of time. *$P <$ 0.05.

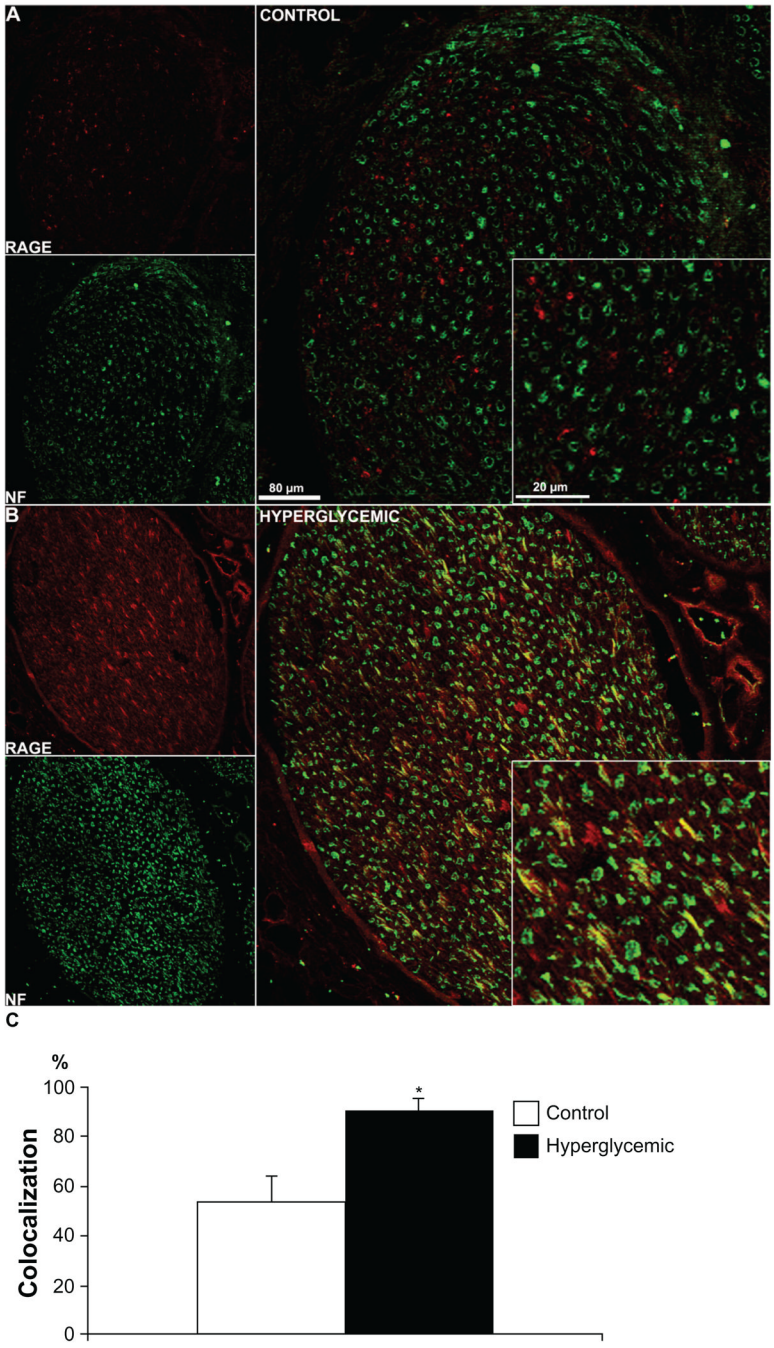

Figure 4.

Neuronal RAGE staining. Confocal images of double immunostaining of RAGE (red) with the neuronal marker, Neurofilament (NF, green). Colocalization of RAGE and NF is very low in the control tissue (**A**), but it is observed in the diabetic tissue (**B**), suggesting that RAGE presence might be largely limited to Schwann cells in sciatic nerves of healthy animals but it is localized to nerve fibers in the hyperglycemic animals. As expected under hyperglycemic conditions, an increase in RAGE staining is not only observed in the nerve but also in surrounding blood vessels (**B**). The quantitative analysis of the colocalization pattern revealed significant difference in number of RAGE positive fibers co-stained for NF between control and hyperglycemic animals (**C**). **P* < 0.03.

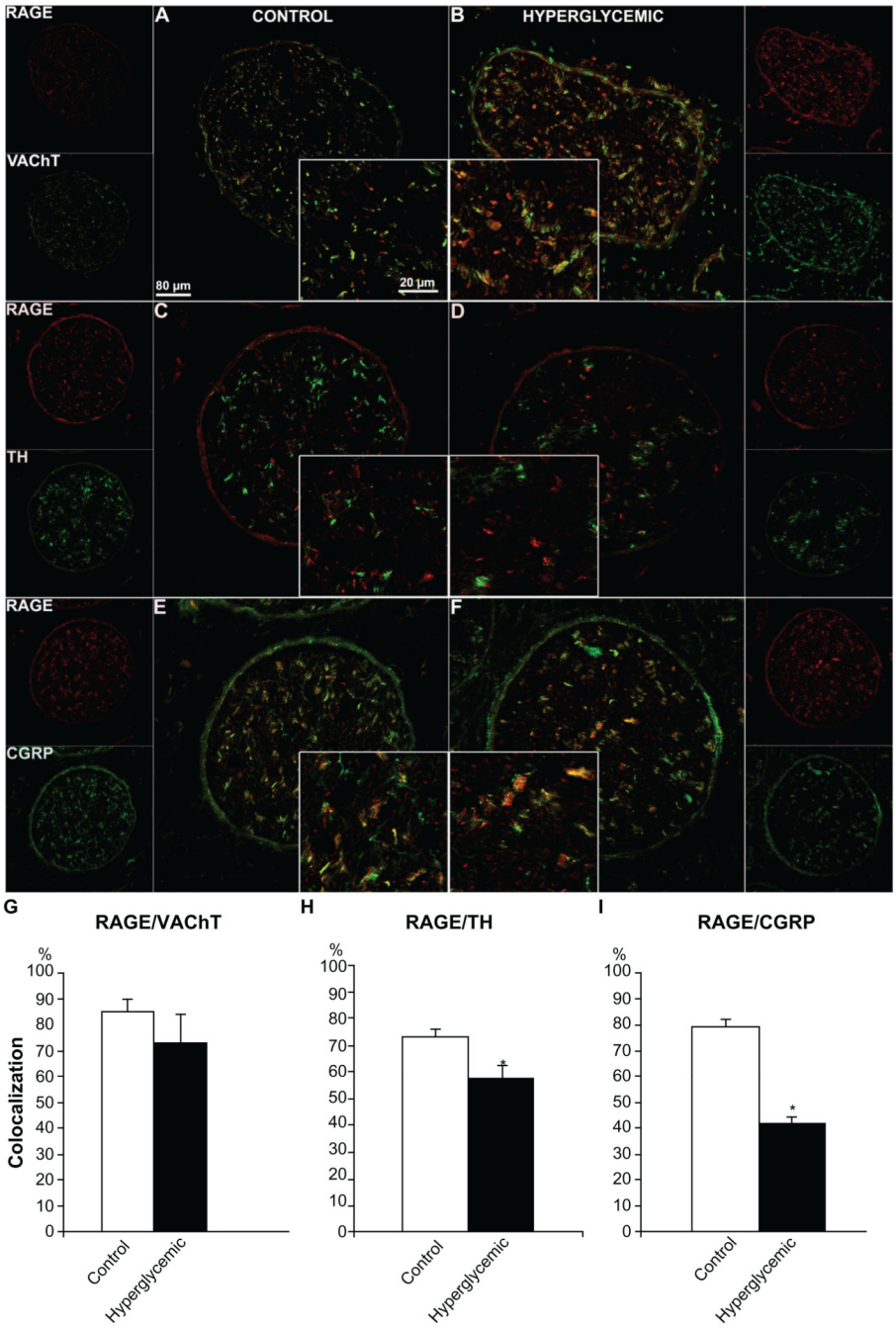

Figure 5.

Immunofluorescence analysis of RAGE distribution in different types of sciatic nerve fibers. Control and diabetic sciatic nerve tissues were subjected to RAGE (red) co-immunostaining with VAChT (motor neuron marker, **A, B**, green), TH (autonomic neuron marker, **C, D**, green) and CGRP (sensory neuron marker, **E, F**, green). Overlay images show that RAGE is localized in all types of sciatic nerve fibers. Note that the perineurial immunofluorescence was non-specific as observed in control staining with the secondary antibody alone. The quantitative analysis of the colocalization pattern revealed that although the number of double stained RAGE/VAChT positive fibers was similar in both groups of animals, there was a significantly lower number of RAGE/TH and RAGE/CGRP positive fibers between

control and diabetic animals (**G, H, I**), supporting our earlier morphological findings on autonomic and sensory fiber loss in diabetic nerve. *$P < 0.001$.

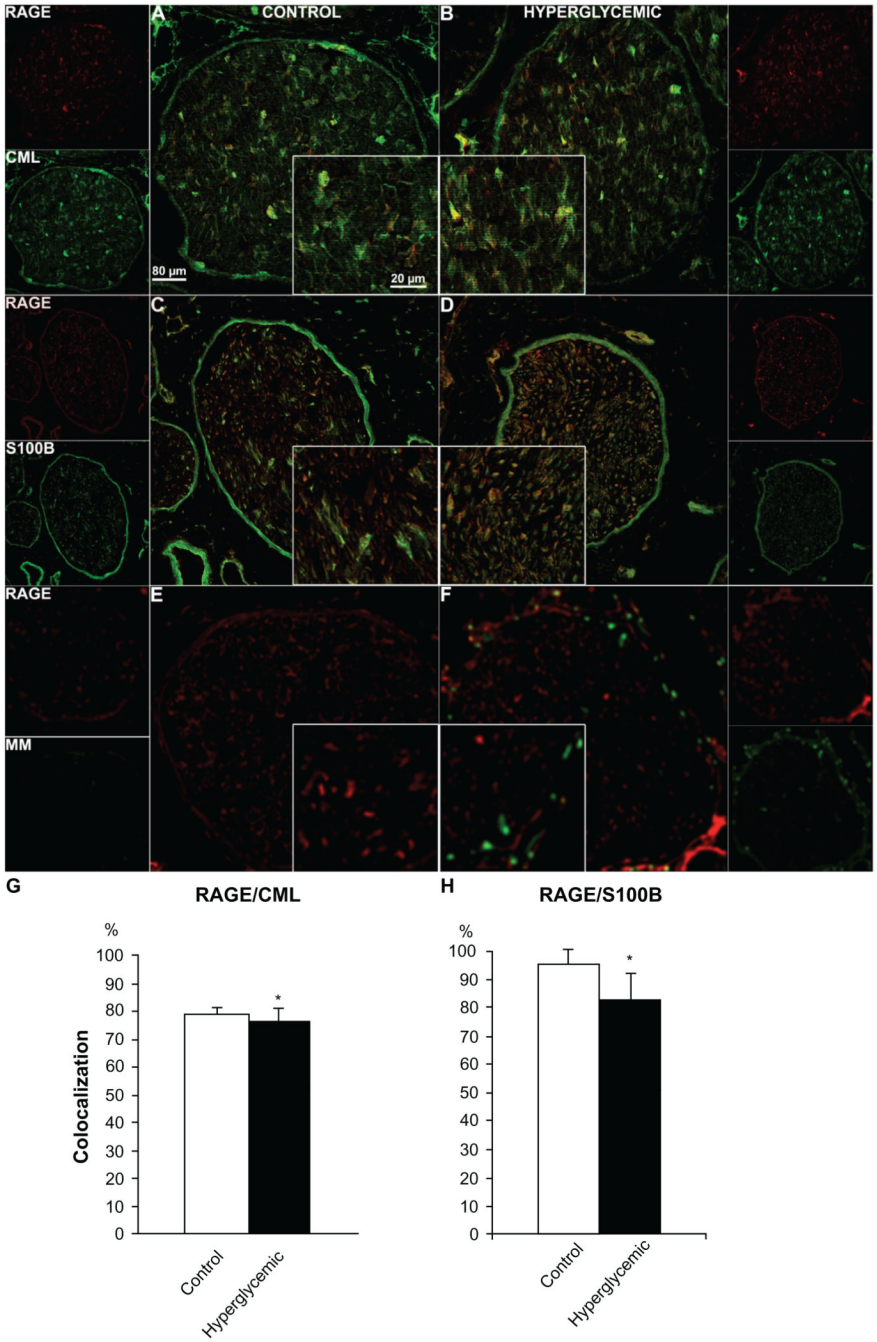

Figure 6.

Colocalization of RAGE and its ligands S100B and CML and RAGE co-expression with macrophage marker (MM). Sciatic nerve sections from control and diabetic animals were subjected to RAGE (red) co-immunostaining with CML (Carboxymethyl Lysine, **A, B**, green), S100B (ligand/Schwann cell marker, **C, D**, green), MM (macrophage marker, **E, F**, green). The quantitative analysis of the colocalization pattern revealed that there was a significant difference in number of RAGE/S100B positive fibers between control and hyperglycemic animals (**G, H**). **P* < 0.001.

Table 1

Hematological and biochemical parameters were measured to assess physiological status of diabetic animals. Similarly to human diabetic patients, pigs with hyperglycemia also exhibit hyperlipidemia. Detailed statistical analysis in Material and Method section.

Substance	Initial (pre-STZ)	1 month	2 months	3 months	Reference values*
Glucose (mmol/l)	2.91 ± 0.16	22.76 ± 1.27	22.6 ± 1.27	24.01 ± 1.34	1.50–3.5
Hemoglobin (mmol/l)	6.79 ± 0.25	5.70 ± 0.19	5.74 ± 0.09	5.85 ± 0.13	5.5–10.4
BUN (mmol/l)	2.59 ± 0.42	5.96 ± 0.69	6.74 ± 6.74	6.19 ± 1.26	0.70–7.85
Creatinine (μmol/l)	53.04 ± 9.72	54.80 ± 3.27	67.18 ± 9.72	74.26 ± 13.23	106–180
GGT (U/l)	47.33 ± 6.5	61.16 ± 1.9	71.5 ± 13.56	69.5 ± 10.72	14–34
Cholesterol (mmol/l)	2.73 ± 0.14	6.35 ± 1.31	6.95 ± 1.54	8.96 ± 1.54	1.3–2.6
Triglyceride (mmol/l)	0.65 ± 0.14	1.19 ± 0.48	2.33 ± 0.88	2.85 ± 1.17	0.2–0.65
LDL (mmol/l)	1.56 ± 0.22	3.72 ± 1.12	4.47 ± 1.156	5.03 ± 1.11	0.6–2
HDLD (mmol/l)	0.87 ± 0.11	2.29 ± 0.13	2.37 ± 0.14	2.51 ± 0.03	0.6–2

*Swindel M. Appendix. Hematology and Serum Chemistry. In: Swindel M, *Swine in the laboratory: Surgery, Anaesthesia, Imaging and Experimental Techniques. 2nd ED,* CRC Press; 2007:409 Bollen PJ. Hansen AK, Rasmusen HJ. Important Biological Features. Normative Values. In: *The laboratory swine.* CRC Press, 2000: 14. Winnicka A. *Reference Values of common laboratory tests in veterinary medicine* (In Polish). Warszawa, Poland. Wydawnictwo SGW. 1997 Holevet et al. *Arterioscler Thromb Vasc Biol.* 1998;18:415–22 (and references within).

Biochem Insights. Author manuscript; available in PMC 2011 August 16.